

Caustics of Catadioptric Cameras *

Rahul Swaminathan, Michael D. Grossberg and Shree K. Nayar

Department of Computer Science, Columbia University
New York, New York 10027

Email: {srahul, mdog, nayar}@cs.columbia.edu

Abstract

Conventional vision systems and algorithms assume the camera to have a single viewpoint. However, sensors need not always maintain a single viewpoint. For instance, an incorrectly aligned system could cause non-single viewpoints. Also, systems could be designed to specifically deviate from a single viewpoint to trade-off image characteristics such as resolution and field of view. In these cases, the locus of viewpoints forms what is called a caustic. In this paper, we present an in-depth analysis of caustics of catadioptric cameras with conic reflectors. Properties of caustics with respect to field of view and resolution are presented. Finally, we present ways to calibrate conic catadioptric systems and estimate their caustics from known camera motion.

1 Introduction

Traditionally, imaging systems have been designed to maintain a single viewpoint. In other words, all the rays of light entering the camera intersect at single point called the effective pinhole. This pinhole model is extensively used in vision algorithms. The single viewpoint is not limited to lens based (dioptric) cameras alone. Catadioptric cameras have also been designed with the aim of maintaining a single effective viewpoint.

Single viewpoint catadioptric cameras include multi-sensor planar mirror systems for panoramic imaging [19] as well as for stereo applications [12]. Curved mirrors have also been used, such as hyperbolic [24, 28] and parabolic [20, 1, 23]. These systems consist of a perspective or telecentric¹ lens and a reflector. The pinhole of the lens is positioned at one of the focal points of the reflector, making the other focal point the effective viewpoint. However, such systems require precise assembly of the imaging components, failing which the viewpoint deviates from a single viewpoint.

Cameras need not always meet the single viewpoint constraint. It is known that relaxing this constraint, gives

greater flexibility in designing imaging systems. Thus, if we allow for deviations from a single viewpoint we could possibly trade-off image characteristics such as field of view and spatial resolution. Catadioptric cameras not having a single view point include: the spherical and conical reflector based designs [15, 27, 26, 3, 18, 8, 9, 4, 10]. Also, in [21], a conical mirror system was proposed to capture a high resolution 360×360 degree stereo panorama.

When an imaging system does not maintain a single viewpoint, a locus of viewpoints in three dimensions is formed, called a caustic [5]. For dioptric systems this is termed as a *diacaustic* and for catadioptric systems as a *catacaustic*. The caustic represents the envelope of all incoming scene rays which are eventually imaged. Each pixel in the image maps to a point on the caustic surface. Understanding caustics aids in the study of the camera's characteristics such as resolution and field of view. One can also imagine cameras designed to possess desirable viewpoint loci. For instance, in [1] the caustic was restricted to a single point. In [22] a stereo sensor was designed by constraining the caustic of the camera to be a circle. Also, sensors have been designed to provide near-perspective projection for a given plane in the scene (see [14]).

In this paper, we study caustics of conic catadioptric systems. By this we mean that the profile of the mirror is a conic section. Conic reflectors based cameras are widely used in vision as well as in astronomical applications. It is therefore interesting to analyze the viewpoint loci of such cameras, when they do not maintain a single viewpoint. In particular we raise the following two questions:

- What happens to the viewpoint locus when a system deviates from a single viewpoint? Note that inspite of using a perspective lens, the catadioptric system need not have a single viewpoint. Instead, the viewpoint locus is described by a three dimensional caustic surface.
- Is there a simple way to estimate the viewpoint loci for such non-single viewpoint systems? Here we present a simple technique to numerically compute the caustic surface using known camera motion and point correspondences between two images.

*This work was supported in parts by a National Science Foundation ITR Award, IIS-00-85864, and the DARPA Human Identification (HiD) Program, Contract No N00014-00-1-0929. The authors thank Prof. P. J. Giblin of the University of Liverpool for useful discussions on caustics.

¹A telecentric lens yields an orthographic projection of the scene onto the image detector.

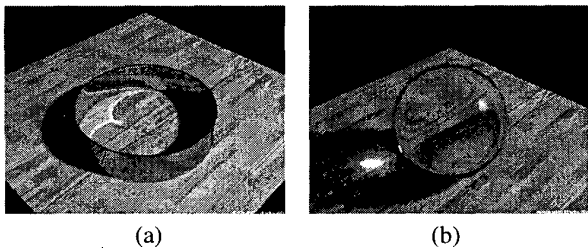


Figure 1: Bright patterns of light on the table illustrate a section of the caustic surface formed. These bright patterns are due to the close bunching together of light rays near the caustic’s surface. The caustics formed are due to light interacting with (a) a metal ring and (b) a spherical refractive element. (Adapted from [16])

To answer these questions, we begin by deriving the caustic surface for a family of conic catadioptric systems. By careful parameterization of the reflector profile, we present a simple derivation of the viewpoint locus as a three-parameter family of curves. These caustic surfaces are then analyzed for their effect on resolution, field of view, and geometric singularities. It should be noted that in this analysis we consider the principal rays passing through the entry pupil of the camera lens to describe the geometry of the sensor. Secondary effects such as blurring do not interfere with the geometric analysis we present. Finally, we present a simple self-calibration technique to estimate the caustic surface numerically for a catadioptric camera using known camera motion.

2 Caustics: Loci of Viewpoints

When a light ray interacts with either a reflective or refractive interface, it may bend and thus alter its path. The envelope of these reflected or refracted rays is called the caustic surface [13, 5]. Caustics formed by reflecting elements are called *catacaustics* and those by refractive elements are called *diacaustics*. Fig.1 illustrates caustics formed by (a) reflection by a metal ring and (b) refraction through a transparent sphere. Near the envelope surface (caustic), the rays of light bunch up together, thus forming bright patterns as seen in the images. Henceforth, we use the term caustic to mean both, the catacaustic as well as the diacaustic.

With respect to imaging devices, caustics represent their loci of viewpoints. The single viewpoint is a degenerate case of a point caustic. Each point on the caustic surface represents the three-dimensional position of a viewpoint and its viewing direction. Thus, the caustic completely describes the geometry of the camera. Hence, one can represent compound imaging systems consisting of multiple components, such as lenses and reflectors, by simply their caustics.

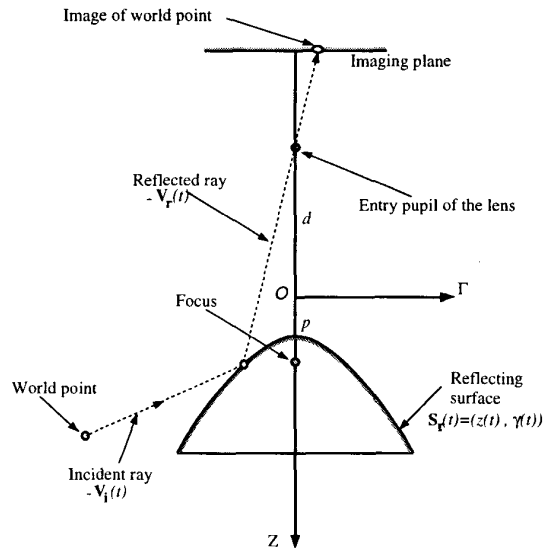


Figure 2: An imaging system consisting of a conic reflector and a perspective lens based camera. The entry pupil of the lens is located at a distance d from the origin, along the axis of symmetry of the conic section. The reflector profile is also defined in this coordinate frame. A light ray from the scene reflects off the reflector surface and is imaged after passing through the entry pupil. A telecentric lens is modeled by taking the limit as $d \rightarrow \infty$. This imaging system can have a non-single viewpoint inspite of using a perspective lens.

2.1 Computing the Caustic

We now study caustics of catadioptric imaging systems consisting of a perspective or telecentric lens and a single reflector whose profile is a conic section. Although, we use the perspective or orthographic projection model for the lens, the imaging system as a whole need not maintain a single viewpoint. We present caustics of rotationally symmetric catadioptric systems, where the entry pupil of the lens is located along the axis of symmetry of the reflector (see Fig.2) at a distance d from the origin O . The reflector profile is also defined in this coordinate frame. Telecentric lenses are modeled by taking the limit $d \rightarrow \infty$.

Many techniques have been proposed to derive the caustics of reflecting and refractive systems including ones based on local conic approximations [6] and the Jacobian method [7]. In our approach we derive the caustic surface based on the Jacobian approach.

2.1.1 The Reflector Surface

Parameterization of the reflector surface is an essential step towards computing the caustic surface analytically. Indeed, whatever the parameterization for the reflector, a solution for the caustic surface exists. We found that standard pa-

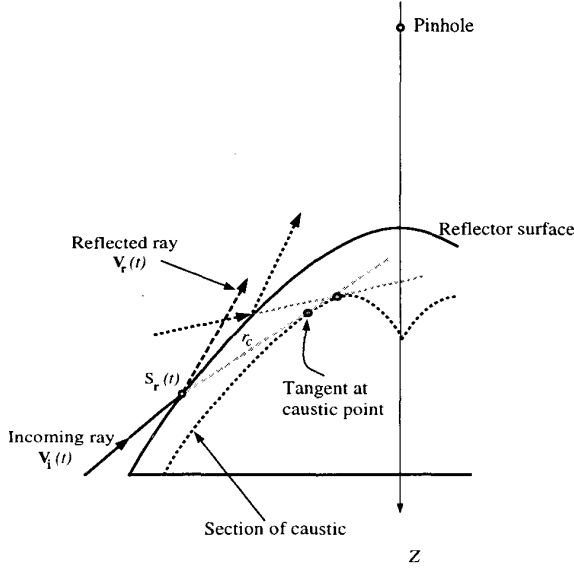


Figure 3: Section of the reflector showing incident rays from the scene reflecting into the lens. The incident ray $\mathbf{V}_i(t)$ is tangential to the caustic surface. The distance of the point on the caustic from the point of reflection is denoted by r_c . At the caustic point if we travel infinitesimally along $\mathbf{V}_i(t)$, we would also move from one ray onto the next. This is due to the close bunching of extended incoming rays at the caustic surface.

parameterizations used for conics, lead to complicated solutions that are difficult to analyze. In contrast, the following generic parameterization yields a simple solution for the caustic surface. Referring to Fig.2, we define:

$$\begin{aligned} z(t) &= t \\ \gamma(t) &= \sqrt{(e^2 - 1)t^2 + 2pt - p^2} \end{aligned} \quad (1)$$

where, e is the eccentricity and p the focus of the conic section. This represents elliptic ($e < 1$), parabolic ($e = 1$) and hyperbolic ($e > 1$) reflectors. The vertex of the reflector is given by $\frac{p}{1+e}$. The Γ -axis is the directrix of the conic reflector. A point on the reflector surface is then $\mathbf{S}_r(t) = [z(t), \gamma(t)]$. Although this parameterization has a singularity for spherical reflectors, it lends itself to a simple analysis of the properties of the family of caustics.

2.1.2 The Caustic Surface

From Fig.2, the vector along the reflected ray (entering the lens pupil) is given by:

$$\mathbf{V}_r(t) = [t + d, \sqrt{(e^2 - 1)t^2 + 2pt - p^2}]. \quad (2)$$

Since we know the geometry of the reflector, its surface normals $\mathbf{N}_r(t)$ can be found analytically. We then derive the pencil of incident rays $\mathbf{V}_i(t)$ from the reflection equation:

$$\mathbf{V}_i(t) = \mathbf{V}_r(t) - 2\mathbf{N}_r(t) (\mathbf{N}_r(t) \cdot \mathbf{V}_r(t)). \quad (3)$$

A point along the incident ray (along $\mathbf{V}_i(t)$), parameterized by its distance r from the point of reflection $\mathbf{S}_r(t)$, is then given by: $\mathbf{S}_r(t) + r \cdot \mathbf{V}_i(t)$. The caustic is tangential to the ray along $\mathbf{V}_i(t)$ and hence for some r_c the caustic point lies at (see Fig. 3):

$$\mathbf{S}_r(t) + r_c \cdot \mathbf{V}_i(t). \quad (4)$$

At this point, the light rays bunch up close together to form an envelope. Thus, in the limit, traversing infinitesimally along $\mathbf{V}_i(t)$ at the caustic, is equivalent to traversing from one ray to the next.

Therefore, at the caustic surface, the determinant of the Jacobian $J(\mathbf{S}_r(t) + r_c \cdot \mathbf{V}_i(t))$ must vanish (see [7]). Let us now denote the Z and Γ components of $\mathbf{S}_r(t)$ by $\mathbf{S}_r(t)_z$ and $\mathbf{S}_r(t)_\gamma$, respectively, and those of $\mathbf{V}_i(t)$ by $\mathbf{V}_i(t)_z$ and $\mathbf{V}_i(t)_\gamma$. Enforcing the vanishing constraint on Eq.4 we get:

$$\det \left(\begin{bmatrix} \dot{\mathbf{S}}_r(t)_z + r_c \cdot \dot{\mathbf{V}}_i(t)_z & \mathbf{V}_i(t)_z \\ \dot{\mathbf{S}}_r(t)_\gamma + r_c \cdot \dot{\mathbf{V}}_i(t)_\gamma & \mathbf{V}_i(t)_\gamma \end{bmatrix} \right) = 0 \quad (5)$$

where, $\dot{\mathbf{S}}_r(t) = \frac{d\mathbf{S}_r(t)}{dt}$ and $\dot{\mathbf{V}}_i(t) = \frac{d\mathbf{V}_i(t)}{dt}$. Solving for r_c we get:

$$r_c(t) = \frac{\dot{\mathbf{S}}_r(t)_\gamma \mathbf{V}_i(t)_z - \dot{\mathbf{S}}_r(t)_z \mathbf{V}_i(t)_\gamma}{\dot{\mathbf{V}}_i(t)_z \mathbf{V}_i(t)_\gamma - \dot{\mathbf{V}}_i(t)_\gamma \mathbf{V}_i(t)_z} \quad (6)$$

Substituting Eq. (6) in Eq. (4), we get the caustic profile for the family of symmetrically positioned conic reflectors and perspective lenses, as a three parameter (e, p, d) family of curves:

$$z_c = \frac{N_z}{D_c}, \quad (7)$$

$$\gamma_c = \frac{N_\gamma}{D_c}, \text{ where,}$$

$$\begin{aligned} N_z &= 2p^3(d+p)^2 + 6(d(e^2-1)-p)p^2(d+p)t \\ &\quad + 3p(d+p)(d(2-3e^2+e^4)+2p)t^2 + \\ &\quad (d^2(e^2-2)(e^2-1)^2 - d(4-7e^2+3e^4)p \\ &\quad + 2(e^4+e^2-1)p^2)t^3, \end{aligned}$$

$$N_\gamma = 2(d+p)(d-de^2+p+e^2p) \\ ((e^2-1)t^2+2pt-p^2)^{\frac{3}{2}},$$

$$\begin{aligned} D_c &= e^2(2(d-p)p^2(d+p)+6p^2(d+p)t \\ &\quad + 3(e^2-1)p(d+p)t^2 + (e^2-1) \\ &\quad (d(e^2-1)-p)t^3). \end{aligned}$$

The caustic produced due to a telecentric lens and a conic reflector is obtained by taking the limit $d \rightarrow \infty$:

$$z_c^\infty = (2p^3 + 6(e^2-1)p^2t + 3(2-3e^2+e^4)pt^2 + (e^2-2)(e^2-1)^2t^3)/(2e^2p^2), \quad (8)$$

$$\gamma_c^\infty = ((1-e^2)((e^2-1)t^2+2pt-p^2)^{\frac{3}{2}})/(e^2p^2).$$

We observe from Eq.(7) that the caustic surface is dependant on the distance d of the entry pupil with respect to the reflector. Now, at what distance d_0 of the pupil, would the system produce a point caustic at the focus $(p, 0)$ of the reflector? From Eq.(7) we set $z_c = p$, and $\gamma_c = 0$ and solve for d_0 :

$$d_0 = p \frac{e^2 + 1}{e^2 - 1} \quad (9)$$

From Eq.(9), setting $e = 1$ (parabolic reflector) gives $d_0 = \infty$, implying the use of a telecentric lens as in [20]. Solutions for elliptical ($e < 1$) and hyperbolic ($e > 1$) reflectors suggest the use of perspective lenses, located at the focal point of the reflectors. Thus, using the caustic surfaces derived above, we can describe single viewpoint systems as a special case of the general solution.

2.2 Examples of Caustic Surfaces

We now present the viewpoint loci for typical catadioptric systems. Figures 4(a), (d) and (g) illustrate viewpoint loci (gray curves), for a catadioptric sensor consisting of a perspective lens and an elliptic, a parabolic and an hyperbolic reflector (dark curves), respectively. The dotted curves in Fig.4(a) denote the part of the elliptic reflector that is self-occluded as well as its corresponding "virtual-caustic". Similarly, Fig.4 (b), (e) and (h) show profiles for catadioptric systems consisting of a telecentric lens and an elliptic, parabolic and hyperbolic reflector, respectively. Note that in Fig.4(e), the caustic degenerates to a point as expected.

Fig.4(c) is a three-dimensional plot of the caustic surface for a symmetric system consisting of a parabolic reflector and a perspective lens. Fig.4(f) depicts the caustic surface in three dimensions for an asymmetric (pupil not on axis of symmetry) catadioptric system. We have described details of how the caustic surface is derived in the asymmetric case in [25]. Fig.4(i) is the viewpoint locus for a catadioptric system including a hyperbolic reflector and a telecentric lens. Unlike the other caustic surfaces that are bounded by their reflector's sizes, this caustic surface expands radially. Thus, if we assumed the system to have a single viewpoint, the perspective image computed for close by scenes is likely to have strong non-perspective distortions, due to parallax between viewpoints.

3 Properties of Caustic Surfaces

We now present some characteristic properties of caustics such as surface singularities and field of view and their relevance to the design of imaging systems.

3.1 Singularities on the Caustic Surface

As seen from Fig.5(a), caustic surfaces have singularities which we refer to as cusps. These correspond to the points on the reflector where its surface normal coincides with the

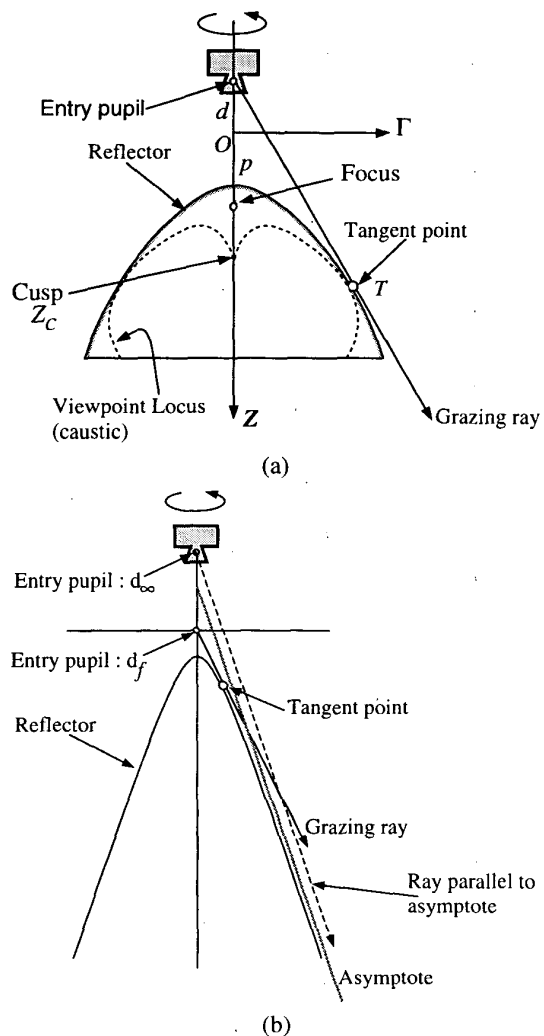


Figure 5: (a) Typical catadioptric camera consisting of a reflector and a perspective lens. The caustic has a singularity denoted by Z_c which we call the cusp. Also shown is the tangent ray to the reflector surface. The point of tangentiality T is also a point on the caustic surface. (b) A catadioptric system consisting of a hyperbolic reflector. A entry pupil at d_f possesses a ray which is tangential to the hyperbola at a finite point. However, no light ray entering the pupil d_∞ can be tangential to the reflector.

reflected light ray (along $\mathbf{V}_r(t)$) entering the lens pupil (see Fig.5(a)). This constraint is given by:

$$\mathbf{V}_r(t) = -\mathbf{N}_r(t). \quad (10)$$

For rotationally symmetric systems with convex or concave reflectors, the cusp lies along the optical axis. Referring to Fig.5(a), we only need to compute the Z coordinate of the cusp. From Eq.(7) and Eq.(10), the Z coordinate of the cusp

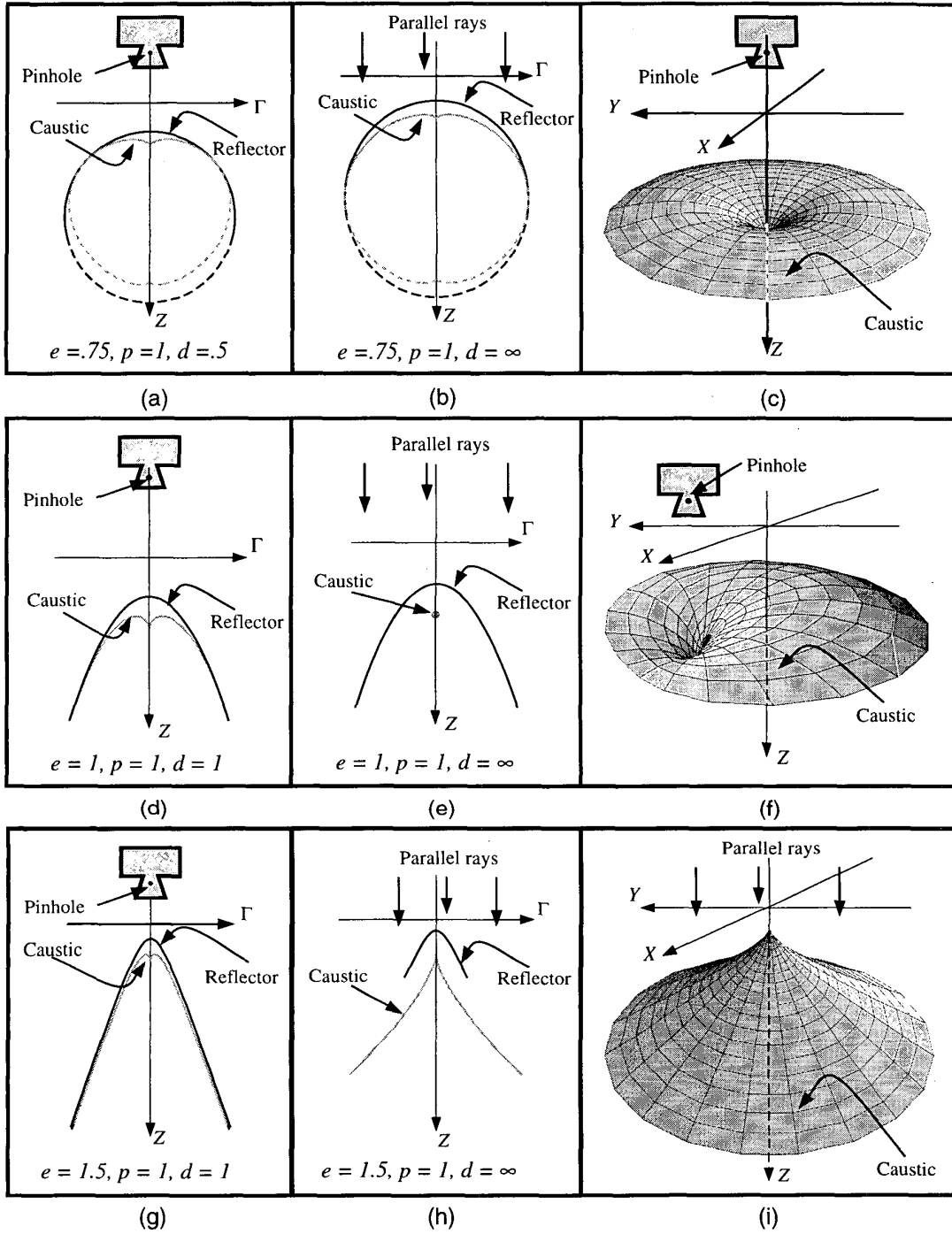


Figure 4: Viewpoint loci for conic catadioptric systems. Column one: Caustics for symmetric systems consisting of a perspective lens and an (a) elliptic, (d) parabolic and (g) hyperbolic reflector. Column two: Viewpoint loci for catadioptric systems consisting of a telecentric lens and an (b) elliptical, (e) parabolic and (h) hyperbolic reflector. Column three: (c) Caustic surface in 3D for a symmetric catadioptric system consisting of a parabolic reflector and perspective lens. (f) Caustic surface for an asymmetric catadioptric camera consisting of an off-axis perspective lens and a parabolic reflector. (i) Caustic surface for a telecentric and hyperbolic reflector system. All caustics were derived using the Jacobian technique described in Section 2.

is given by:

$$Z_c = \frac{p((1+e)(2+e+e^2)d + 2(1+e+e^2)p)}{(1+e)(2(1+e)d + (2+e+e^2)p)}. \quad (11)$$

We now discuss the significance of the cusp in the design of sensors. *At what point in 3D, can we best approximate the locus of viewpoints by a single point?* From the symmetry of the system, we restrict this point to lie on the optical axis. This still leaves us with infinite possibilities. However, the lens' entry pupil and the cusp point, together give us finite bounds between which it makes sense to place the approximate single viewpoint. Further, in Eq.(11), taking the limit $d \rightarrow \infty$, we find that the position of the cusp converges to:

$$Z_c^\infty = \frac{p(2+e(1+e))}{2(1+e)}. \quad (12)$$

Thus, even if the exact location of the entry pupil is unknown, one can estimate an upper bound on the cusp's location. This bound can be used in practice to estimate the "best" location to approximate the caustic by a point.

3.1.1 Caustics and Field of View

Catadioptric systems consisting of convex reflectors have a pencil of rays which graze the reflector surface (see Fig. 5 (a)). These rays define the limit of the field of view of the camera. For convex reflectors, the point of tangentiality of the grazing ray is also its corresponding caustic point (see [25]). Thus, the distance of the caustic point from the reflector surface is zero or $r_c = 0$. By setting Eq.(6) to be zero, we solve for the point of tangentiality, $t_{r=0}$:

$$t_{r=0} = \frac{p(d+p)}{d+p-de^2}, \quad (13)$$

which is a useful bound on the size of the viewpoint locus.

It should be noted that hyperbolic mirrors do not always have a grazing ray because the reflector is asymptotic. If the perspective lens is placed between the vertex of the reflector and the point of intersection between its two asymptotes, a tangent ray (grazing ray) exists which touches the reflector at a finite point, giving a finite caustic surface. In contrast, if the lens were placed further away, there exists no ray that grazes the reflector surface (see Fig.5 (b)). The caustic of such an imaging system is asymptotic, and approaches the reflector surface.

4 Resolution

In [2], conic reflector based single viewpoint catadioptric cameras were shown to possess radially increasing resolution. We now investigate the resolution characteristics of catadioptric systems in general. The results derived below apply to single viewpoint as well as non-single viewpoint systems.

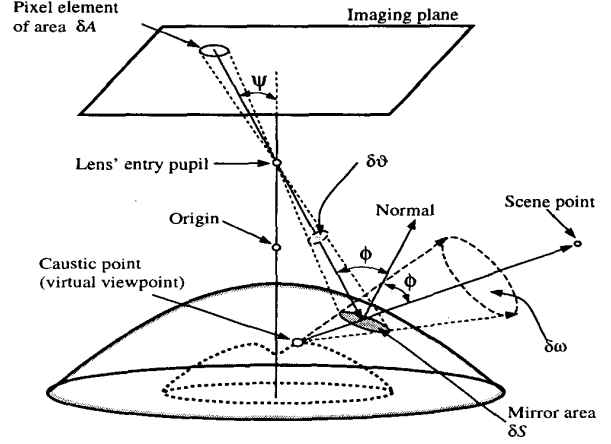


Figure 6: A pixel element of area δA in the image plane projects through the entry pupil of the lens onto the reflector as a region of area δS . The pupil is located at $(0, 0, d)$, with respect to the origin. The principal ray from δA reflects off the reflector at $s_R(x(t, \theta), y(t, \theta), z(t, \theta))$. The corresponding viewpoint on the caustic surface is as shown above. The solid angle subtended at this viewpoint is then $\delta\omega = \delta S/r_c^2$, where r_c is the distance of the viewpoint from the reflector (see Eq.(6)). Resolution is then defined as a ratio of $\delta\omega$ to δA .

4.1 Single Reflector with Perspective Lens

Consider an infinitesimal area δA in the imaging plane which makes an angle ψ with the optical axis (see Fig. 6). Let this area image an infinitesimal solid angle $\delta\omega$ of the scene. The resolution is then defined as: $\frac{\delta A}{\delta\omega}$.

The solid angle subtended at the entry pupil of the lens is given by $\delta\vartheta = \delta A \cos^3(\psi)/f^2$, where f is the focal length of the lens. The area projected onto the reflector by δA is then:

$$\delta S = \frac{\delta A \cos(\psi)(d + x_c(t))^2}{(f^2 \cos(\phi))}, \quad (14)$$

where, ϕ is the angle between the principal ray corresponding to δA and the surface normal at δS . The foreshortened area visible to the viewpoint (of the principal ray) on the caustic surface is $\delta A \cos(\psi)(d + x_c(t))^2/f^2$. The solid angle subtended at this viewpoint is given by:

$$\delta\omega = \frac{\delta A \cos(\psi)(d + x_c(t))^2}{f^2 \cdot r_c^2}, \quad (15)$$

where, r_c is the distance of the viewpoint from the reflector surface as defined in Eq.6. For conic catadioptric systems, resolution is then defined as:

$$\frac{\delta A}{\delta\omega} = \frac{f^2 \cdot r_c^2}{\cos(\psi)(d + z(t))^2}. \quad (16)$$

Fig. 7 illustrates the resolution across a radial slice of the

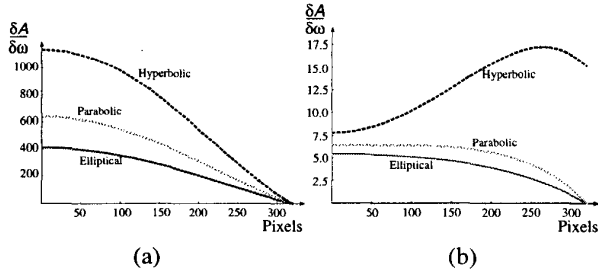


Figure 7: Plots of resolution for catadioptric sensors having a perspective lens based camera and an elliptic, a parabolic and an hyperbolic reflector. The plots illustrate the resolution across a radial slice of the image plane when the pupil is located at (a) the origin ($d = 0$) and (b) at $d = 6$.

imaging plane. The curves have been normalized with respect to magnification such that area of the reflector’s image in all three cases are the same. This facilitates a fair comparison of resolution between the three catadioptric systems. As seen, resolution drops drastically beyond some distance from the image center. However, by careful choice of reflector and geometry of the system, we can take advantage of the initial rise in resolution (see Fig. 7(b)). For instance, we can use only the section of the reflector for which the optical resolution increases.

5 Self Calibration of Caustics

As suggested earlier, caustics completely describe the geometry of an imaging system. Thus, the calibration of a camera is equivalent to estimating its caustic surface. In the past, techniques for calibrating single viewpoint catadioptric systems have been suggested using single images [11] or camera motion [17]. In contrast, our technique also calibrates non-single viewpoint systems by estimating the camera’s caustic surface, using known camera motion and point correspondences between views of unknown scene points.

Since the parameterization in Section 2 is singular for a sphere, we parameterize the reflector surface as:

$$A \cdot z^2 + \gamma^2 + B \cdot z = C, \quad (17)$$

which includes the entire class of conic reflectors. As before, the entry pupil is at a distance d from the origin along the Z axis. The caustic surface is then described by a four-parameter (A, B, C, d) family of curves, derived analytically using the Jacobian method [7] (see [25] for details).

5.1 Objective Function

We pose the caustic estimation problem as one of error minimization. Let p_1 and p_2 be the images of a scene point P , in the two views. From the hypothesized parameter values (during search), we can map p_1 and p_2 to their corresponding viewpoints (S_1 and S_2) as well as their viewing direc-

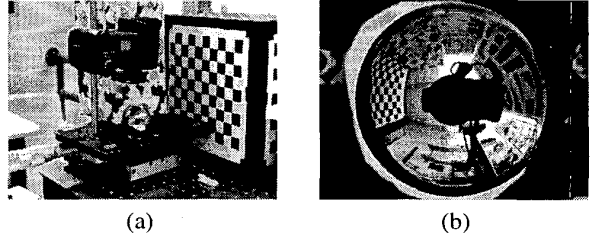


Figure 8: (a) A catadioptric camera consisting of a perspective lens based digital camera and a spherical reflector (ball-bearing). The reflector’s radius is 25.4mm, and lens’ entry pupil is approximately 150mm above the center of the sphere. The catadioptric camera was placed on a translation stage and translated by 20mm along the Y axis. (b) Sample image acquired during the calibration process. Each image is 2048×1536 in size.

tions (V_1 and V_2). We now find in closed form, a point \tilde{P} along the incident ray V_1 which is closest to ray V_2 (this is the best estimate of the scene point P). We define the error function as the disparity between the image of \tilde{P} in the second view (\tilde{p}_2) and p_2 .

5.2 Experimental Results

We tested our algorithm for a catadioptric camera consisting of a perspective lens and a spherical reflector (ball bearing) (see Fig. 8(a)). Fig.8(b) shows a typical image acquired by this catadioptric system. We know the reflector to be spherical and hence we need to estimate only the focal length f of the perspective lens, distance d of the lens’s entry pupil from the reflector, and the radius of the reflector \sqrt{C} .

We used close by scene points for correspondences, since the effect of varying viewpoints diminishes with depth of the scene point. The camera was translated precisely by 20mm sideways (along the Y axis) to get the two views. Using 41 point correspondences, and a non-linear search, we estimated the camera parameters listed in Fig.9. Fig.10 compares the estimated caustic surface (dotted curve) with the ground truth caustic curve (solid curve). The ground truth is based on careful manual measurement of the required parameters. As can be seen, the recovered radius of the reflector is accurate to within a few millimeters. The estimated focal length too is close to the ground truth. However, the estimate of d is a little erroneous. This can be due to incorrect convergence of the search to a local minima as well as from erroneous measurement of ground truth.

	\sqrt{C} (mm)	d (mm)	f (pixels)
Ground Truth	25.4	150	5381
Estimated Values	24.7	176.9	5379

Figure 9: Estimated and ground truth parameters for the catadioptric camera shown in Fig.8. The estimation was done using constrained minimization routines in Matlab.

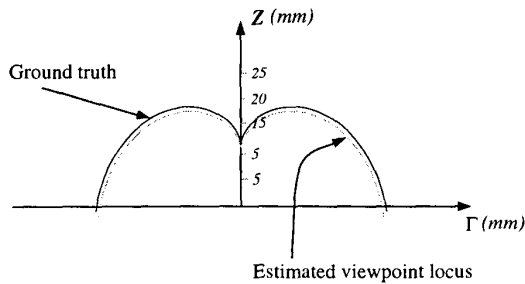


Figure 10: Ground truth (solid curve) and estimated caustic (dotted curve) for the imaging system shown in Fig.8. As seen, the error in the estimated viewpoint locus of the camera is marginal and follows the ground truth caustic closely.

6 Summary

In this paper, we derived a concise analytic form for the loci of viewpoints (caustics) for imaging systems consisting of a conic reflector (whose profile is a conic section) and a perspective or a telecentric lens based camera. We showed that the single viewpoint catadioptric system is a special case under this framework.

Using caustics we analysed the camera for its characteristics like field of view, resolution and geometric singularities, in the most general sense. We also illustrated how resolution degrades radially beyond some distance from the image center, if the effective viewpoint locus is not a single point.

Finally we presented a simple calibration technique to estimate the caustic surface and camera parameters for a conic catadioptric system using known camera motion. Although we assumed knowledge of the reflector shape, the precise geometry of the camera was unknown and was estimated from two images of an arbitrary scene.

References

- [1] S. Baker and S. K. Nayar. A Theory of Catadioptric Image Formation. In *Proc. ICCV*, pages 35–42, 1998.
- [2] S. Baker and S. K. Nayar. A Theory of Single-Viewpoint Catadioptric Image Formation. *IJCV*, 35(2):1–22, November 1999.
- [3] S. Bogner. Introduction to Panoramic Imaging. In *IEEE SMC Conference*, volume 54, pages 3100–3106, October 1995.
- [4] R. C. Bolles, K. G. Konolige, and M. A. Fischler. Extra Set of Eyes. In *DARPA-IUW*, pages 41–44, 1997.
- [5] M. Born and E. Wolf. *Principles of Optics*. Pergamon Press, 1965.
- [6] J. W. Bruce, P. J. Giblin, and C. G. Gibson. On Caustics of Plane Curves. *American Mathematical Monthly*, 88:651–667, November 1981.
- [7] D. G. Burkhard and D. L. Shealy. Flux Density for Ray Propagation in Geometrical Optics. *Journal of the Optical Society of America*, 63(3):299–304, March 1973.

- [8] J. Chahl and M. Srinivasan. Reflective surfaces for panoramic imaging. *Applied Optics*, 36(31):8275–8285, 1997.
- [9] J. Charles, R. Reeves, and C. Schur. How to build and use an all-sky camera. *Astronomy Magazine*, April 1987.
- [10] S. Derrien, and K. Konolige. Approximating a single viewpoint in panoramic imaging devices. In *International Conference on Robotics and Automation*, pages 3932–3939, 2000.
- [11] C. Geyer and K. Daniilidis. Catadioptric camera calibration. In *Proc. ICCV*, pages 398–404, 1999.
- [12] J. Gluckman and S. K. Nayar. Planar Catadioptric Stereo: Geometry and Calibration. In *CVPR*, pages I:22–28, 1999.
- [13] W. R. Hamilton. Theory of Systems of Rays. *Transactions of the Royal Irish Academy*, 15:69–174, 1828.
- [14] R. Hicks and R. Bajcsy. Catadioptric Sensors that Approximate Wide-Angle Perspective Projections. In *Proc. CVPR*, pages I:545–551, 2000.
- [15] J. W. Hong, X. Tan, B. Pinette, R. Weiss, and E. M. Riseman. Image-Based Navigation Using 360 Views. In *DARPA-IUW*, pages 782–791, 1990.
- [16] H. W. Jensen. In <http://graphics.stanford.edu/henrik/images/caustics.html>, 1996.
- [17] S. B. Kang. Catadioptric self-calibration. In *Proc. CVPR*, pages I:201–207, June 2000.
- [18] J. Murphy. Application of panoramic imaging to a teleoperated lunar rover. In *IEEE SMC Conference*, volume 36, pages 3117–3121, October 1997.
- [19] V. Nalwa. A True Omnidirectional Viewer. Technical report, Bell Laboratories, Holmdel, NJ 07733, U.S.A., February 1996.
- [20] S. K. Nayar. Catadioptric Omnidirectional Cameras. In *Proc. CVPR*, pages 482–488, 1997.
- [21] S. K. Nayar and A. D. Karmarkar. 360 x 360 Mosaics. In *Proc. CVPR*, pages I:388–395, 2000.
- [22] S. Peleg, Y. Pritch, and M. Ben-Ezraet. Cameras for stereo panoramic imaging. In *Proc. CVPR*, pages I:208–214, June 2000.
- [23] V. N. Peri and S. K. Nayar. Generation of Perspective and Panoramic Video from Omnidirectional Video. *DARPA-IUW*, pages I:243–245, December 1997.
- [24] D. Rees. Panoramic television viewing system. *United States Patent No. 3,505,465*, April 1970.
- [25] R. Swaminathan, M. D. Grossberg, and S. K. Nayar. Non-Single Viewpoint Catadioptric Cameras: Geometry and Analysis. Technical Report CUCS-004-01, Dept. of Computer Science, Columbia University, 2001.
- [26] Y. Yagi, S. Kawato, and S. Tsuji. Real-Time Omnidirectional Image Sensor (copis) for Vision-Guided Navigation. *Robotics and Automation*, 10(1):11–22, February 1994.
- [27] Y. Yagi and M. Yachida. Real-Time Generation of Environmental Map and Obstacle Avoidance Using Omnidirectional Image Sensor with Conic Mirror. In *Proc. CVPR*, pages 160–165, 1991.
- [28] K. Yamazawa, Y. Yagi, and M. Yachida. Omnidirectional imaging with hyperboloidal projection. In *Proc. IEEE/RSJ International Conference on Intelligent Robots and Systems*, pages 1029–1034, July 1993.